Journal of Magnetic Resonance **152,** 48–56 (2001)
doi:10.1006/jmre.2001.2401, available online at http://www.idealibrary.com on IDEAL®

Pure-Phase Selective Excitation in Fast-Relaxing Systems

Klaus Zangger,*,[1] Monika Oberer,† and Heinz Sterk*

*Institute of Chemistry/Organic and Bioorganic Chemistry, and †Division of Physical Chemistry, University of Graz, Heinrichstrasse 28, A-8010 Graz, Austria

Received December 8, 2000; revised June 4, 2001

Selective pulses have been used frequently for small molecules. However, their application to proteins and other macromolecules has been limited. The long duration of shaped-selective pulses and the short T_2 relaxation times in proteins often prohibited the use of highly selective pulses especially on larger biomolecules. A very selective excitation can be obtained within a short time by using the selective excitation sequence presented in this paper. Instead of using a shaped low-intensity radiofrequency pulse, a cluster of hard 90° pulses, delays of free precession, and pulsed field gradients can be used to selectively excite a narrow chemical shift range within a relatively short time. Thereby, off-resonance magnetization, which is allowed to evolve freely during the free precession intervals, is destroyed by the gradient pulses. Off-resonance excitation artifacts can be removed by random variation of the interpulse delays. This leads to an excitation profile with selectivity as well as phase and relaxation behavior superior to that of commonly used shaped-selective pulses. Since the evolution of scalar coupling is inherently suppressed during the double-selective excitation of two different scalar-coupled nuclei, the presented pulse cluster is especially suited for simultaneous highly selective excitation of N–H and C–H fragments. Experimental examples are demonstrated on hen egg white lysozyme (14 kD) and the bacterial antidote ParD (19 kD).

Key Words: **NMR spectroscopy; pulse cluster; pulsed field gradients; relaxation; selective excitation.**

INTRODUCTION

For biological macromolecules, signal overlap in NMR spectra often prevents the extraction of useful parameters, like NOEs, relaxation times, coupling constants, or homonuclear and heteronuclear correlations. Two- and multidimensional experiments can be used to circumvent this resolution problem (*1*). However, in some cases one is interested in only one or a few specific resonances. To overcome the long measurement times and large data storage requirements of multidimensional NMR spectra, selective experiments have been used (*2–6*). Through selective excitation by either shaped low-amplitude radiofrequency pulses (*6*) or DANTE pulse clusters (*7*), the fate of one specific signal during a pulse sequence can be monitored without the influence of other resonances. This also reduces the dimensionality of necessary NMR experiments, since the origin of magnetization is known and no frequency discrimination is necessary in the dimension belonging to the selectively excited spin. So far, the use of selective pulses for proteins has been restricted mainly to applications employing band-selective pulses for, e.g., the excitation of α- or carbonyl carbons in triple-resonance experiments (*8, 9*) or selective pulses for solvent suppression (*10*). An interesting approach to selective excitation for isotopically labeled macromolecules, where magnetization can be selectively excited within a rather short time by using doubly selective cross-polarization, has recently been described (*11–13*). However, this approach is not feasible for unlabeled macromolecules and in situations where the frequency of the heteronuclear scalar coupling partner is unknown.

Generally, the duration of a selective pulse is proportional to the reciprocal of the excitation bandwidth (*3, 14*). For proteins and other macromolecules, the long durations necessary for highly selective pulses would cause substantial loss of magnetization due to relaxation during the application of the shaped pulse. In addition to signal losses, the excitation profiles deteriorate if significant relaxation is present (*14, 15*). This is not surprising, since relaxation is usually not considered in the design of shaped pulses especially when numerical optimization procedures are employed (*16*). However, various selective pulses have been optimized to reduce relaxation losses during the pulse. Some of these are derived by simulated annealing of shaped radiofrequency pulses (*17, 18*), while another one (DANTE-Z) (*19, 20*) belongs to the DANTE pulse family. The favorable relaxation behavior of the latter method stems partially from the storage of selectively excited magnetization along the z-direction after each pulse train.

To obtain highly selective excitation within a short time with an easily implemented pulse sequence, a new excitation scheme that is not based on shaped low-power pulses but instead uses a combination of hard (nonselective) 90° pulses, delays of free precession, and pulsed field gradients to suppress off-resonance magnetization is presented here.

[1] To whom correspondence should be addressed. Fax: 43 316 380-9840. E-mail: klaus.zangger@kfunigraz.ac.at.

1090-7807/01 $35.00

THEORY

The pulse sequences used are shown in Fig. 1. After excitation by the first 90° x pulse, the magnetization is allowed to precess freely during the delay τ_a (Fig. 1a). The next 90° pulse with opposite phase flips the magnetization, which is aligned along the y direction back along the z axis. Magnetization along the x axis is defocused by the subsequent pulsed field gradient. In terms of product operators the first 90° x pulse creates I_y magnetization, which evolves during τ_a under the chemical shift ω_I to give

$$I_y \cos(\omega_I \tau_a) + I_x \sin(\omega_I \tau_a). \quad [1]$$

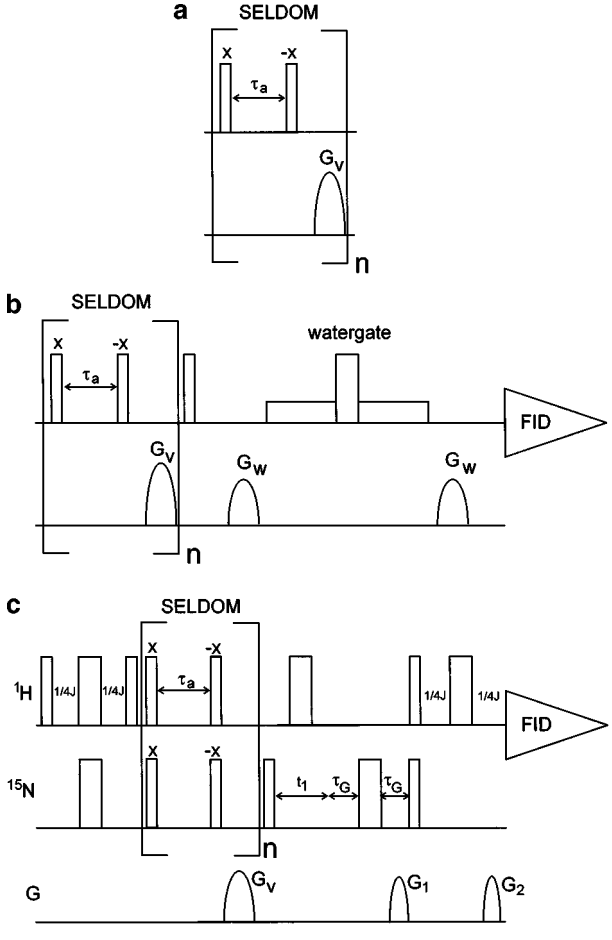

FIG. 1. Pulse sequences of (a) the presented selective excitation pulse cluster, (b) a selectively excited 1D watergate, and (c) an N–H double-selective HSQC. Thin and thick bars represent 90° and 180° pulses, respectively. Only the phases for the SELDOM scheme are shown; the others are as described for the original watergate and HSQC experiments. τ_a is the varying interpulse delay of the SELDOM cluster, t_1 the incrementable delay in the HSQC experiment, and τ_G the delay needed for refocusing the chemical shifts during the application of G_1. The relative strengths of $G_1 : G_2$ are 10 : 1. G_w is the de- and refocusing gradient for the watergate sequence and G_v serves to defocus the magnetization that evolved during τ_a. The latter gradient needs to be changed in a noncorrelated way during successive steps of the SELDOM scheme to prevent refocusing of unwanted off-resonance magnetization.

The next 90°–x pulse flips the I_y term back to the z direction, whereas I_x is unaffected:

$$I_y \cos(\omega_I \tau_a) + I_x \sin(\omega_I \tau_a) \xrightarrow{90°-x} I_z \cos(\omega_I \tau_a) + I_x \sin(\omega_I \tau_a). \quad [2]$$

The subsequently applied z gradient destroys all magnetization left in the x, y plane. Therefore, the amount of off-resonance magnetization destroyed by this pulse cluster is equal to the x component created during the delay $\tau_a (= \sin(2\pi\nu\tau_a))$. This gives a cosine-modulated excitation in the frequency domain according to $\cos(2\pi\nu\tau_a)$. Repeating the sequence several times with varying delays τ_a leads to an averaging of the side loops of the excitation profile and therefore an increasing of the levels of off-resonance signal suppression. On the other hand, on-resonance magnetization is not affected by the gradient and therefore is aligned along the z axis at the end of the selective excitation scheme. This method of selective excitation that we termed SELDOM (*sel*ective excitation by *d*estruction of *o*ff-resonance *m*agnetization) pulse cluster can be used for selective excitation whenever the magnetization is along the z direction. In cases where transverse magnetization is present, it simply must be converted to z magnetization before the application of the presented excitation scheme.

This SELDOM cluster can be used at the beginning of a pulse sequence (Fig. 1b) or for example in the middle of an HSQC experiment (*21*) (Fig. 1c) if the two 90° pulses on the proton and X nucleus, which transfer the magnetization from anti-phase proton to anti-phase X-magnetization, are not executed simultaneously but sequentially. Thereby, $I_z S_z$ magnetization is produced and both the I and S nuclei can be selectively excited. By using regular selective pulses (shaped pulses or DANTE-type clusters) the excitation bandwidth must be large enough to excite the whole H–X doublet since scalar coupling is active during the selective excitation. However, for the proposed selective excitation scheme highly selective excitation is possible since the simultaneous 90° hard pulses on the H and X nucleus produce a combination of double- and zero-quantum magnetization (e.g., $I_x S_x$) and therefore scalar coupling is not active during the delays of free precession τ_a.

The magnetization retained during n successive steps of the selective excitation cluster is given by

$$I = I_0 * \prod_{i=1}^{n} \cos(2\pi\nu\tau_{ai}), \quad [3]$$

where I is the observable signal intensity, I_0 is the signal intensity at the start of the sequence, and τ_{ai} is the ith delay τ_a.

The interpulse delay τ_a can be either randomly or systematically changed between each repetition. The higher the number of repetitions, the better the destruction of off-resonance magnetization. However, to keep relaxation losses to a minimum, the

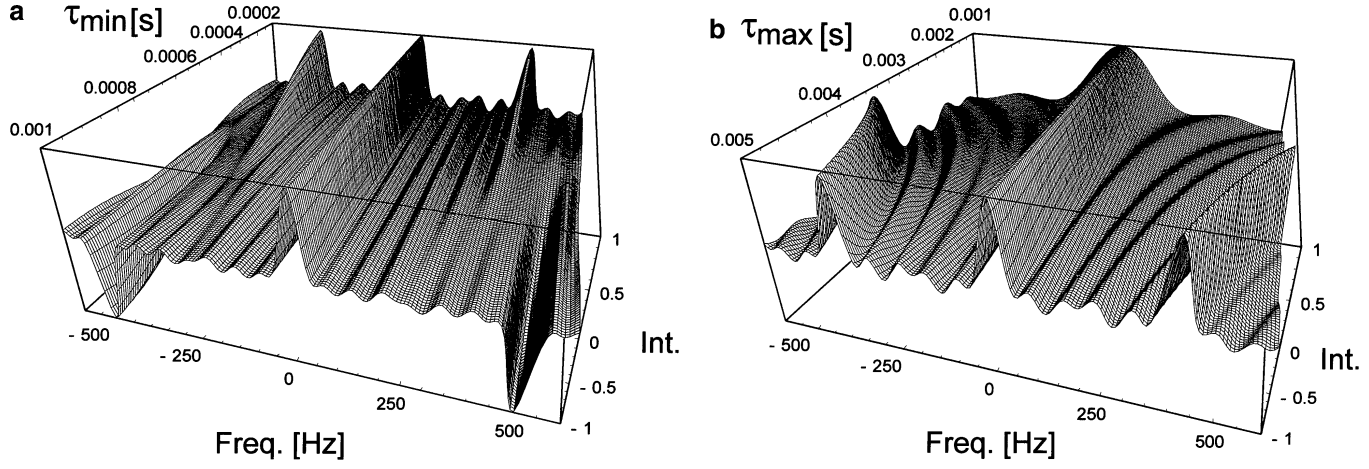

FIG. 2. Excitation profiles calculated with Eq. [3] for (a) constant τ_{max} (= 5 ms) as a function of τ_{min}, and (b) constant τ_{min} (= 0.1 ms) as a function of τ_{max}. Five equally spaced repetitions of the SELDOM pulse cluster were used and the delay τ_a was incremented in equidistant steps. (a) A variation of τ_{min} mainly influences the position and sign of excitation sidebands, whereas (b) a variation of τ_{max} has more significant effects on the excitation bandwidth.

total duration of this excitation scheme should be as short as possible. During the application of the gradients the on-resonance magnetization is along the $+z$ axis and therefore no T_1 and T_2 relaxation losses occur. Some magnetization is lost during the whole pulse cluster through cross-relaxation since the other spins are defocused. However, cross-relaxation also leads to sometimes significantly deteriorated excitation in other selective excitation schemes (*15*). The excitation profile can be calculated for systematic variations of the delay τ_a using Eq. [3]. For a selective excitation using five repetitions and an equidistant incrementation of τ_a between τ_{min} and τ_{max} the calculated excitation profiles are shown in Figs. 2a and 2b for constant τ_{max} (= 5 ms) and τ_{min} (= 0.1 ms) as a function of τ_{min} and τ_{max}, respectively. The excitation bandwidth is mainly determined by τ_{max}, since the evolution of chemical shifts is most pronounced during this interval. As can be seen in Fig. 2b, a shorter τ_{max} leads to broader excitation profiles, whereas a shorter τ_{min} has negligible effects on the excitation bandwidth. Excitation side bands like those seen in Figs. 2a and 2b are produced if the delay τ_a is incremented in equal steps, as explained below and could be suppressed if τ_a is incremented randomly. Excitation artifacts of up to about 15% of maximum signal, which are created by nonoptimal off-resonance signal suppression, can be reduced by using a higher number of repetitions. However, this would require longer durations of this selective excitation scheme. Even more powerful for the reduction of off-resonance signals is randomization of the delay τ_a between individual transients or increments in multidimensional experiments as will be shown in the experimental results. During the individual steps of the SELDOM scheme, zero-quantum terms could be created for scalar coupled nuclei, which would not be defocused by the gradients. However, such coherences can also be eliminated by random variation of the interpulse delays.

It should be noted that the proposed selective excitation scheme is not related to DANTE pulses, which consist of an array of short pulses whose excitation sums up to one 90° pulse, whereas the SELDOM cluster consists of an array of 90° excitations whose off-resonance artifacts are eliminated by the variation of the interpulse delay. Therefore, it can be described as a series of 1–$\bar{1}$ binomial sequences with varying interpulse delays and gradients in between to defocus off-resonance magnetization. A somehow similar way of reducing "excitation sidebands" was presented by Shaka and Freeman (*22*, *23*), who used arrays of "prepulses" of varying pulse angles and phases to suppress harmonic responses in spatially localized *in vivo* experiments, which stem from signals excited in sample regions where the flip angle is around 270°, 450°, etc.

Pure phase-selective excitation has also been achieved by a method termed *excitation sculpting* (*24–26*), where a selective excitation pulse is flanked by two gradients of the same strength and duration and a subsequent repetition of this pulse sandwich with a different gradient strength. This gives a G_1–S–G_1–G_2–S–G_2-type excitation cluster, where G_1 and G_2 are two gradients of varying field strengths and S can be any selective pulse. In this case the excitation bandwidth is still determined by the selective pulse within the sequence and T_2 relaxation of all spins occurs during the application of the pulsed field gradients. The need for applying the selective pulse twice in this sequence further enhances transverse relaxation losses.

RESULTS AND DISCUSSION

Experimental excitation profiles of the presented excitation scheme in comparison with several basic shaped-selective pulses are shown in Fig. 3 in phase-sensitive (Figs. 3a, 3c, 3e, 3g, 3i) and absolute value (Figs. 3b, 3d, 3f, 3h, 3j) representation. For all profiles the duration of the selective pulse was 3.5 ms. Figure 3 clearly shows that in addition to the narrowest excitation bandwidth, the SELDOM cluster (Figs. 3a, 3b) also produces no dispersive components (Fig. 3a), which are very prominent for

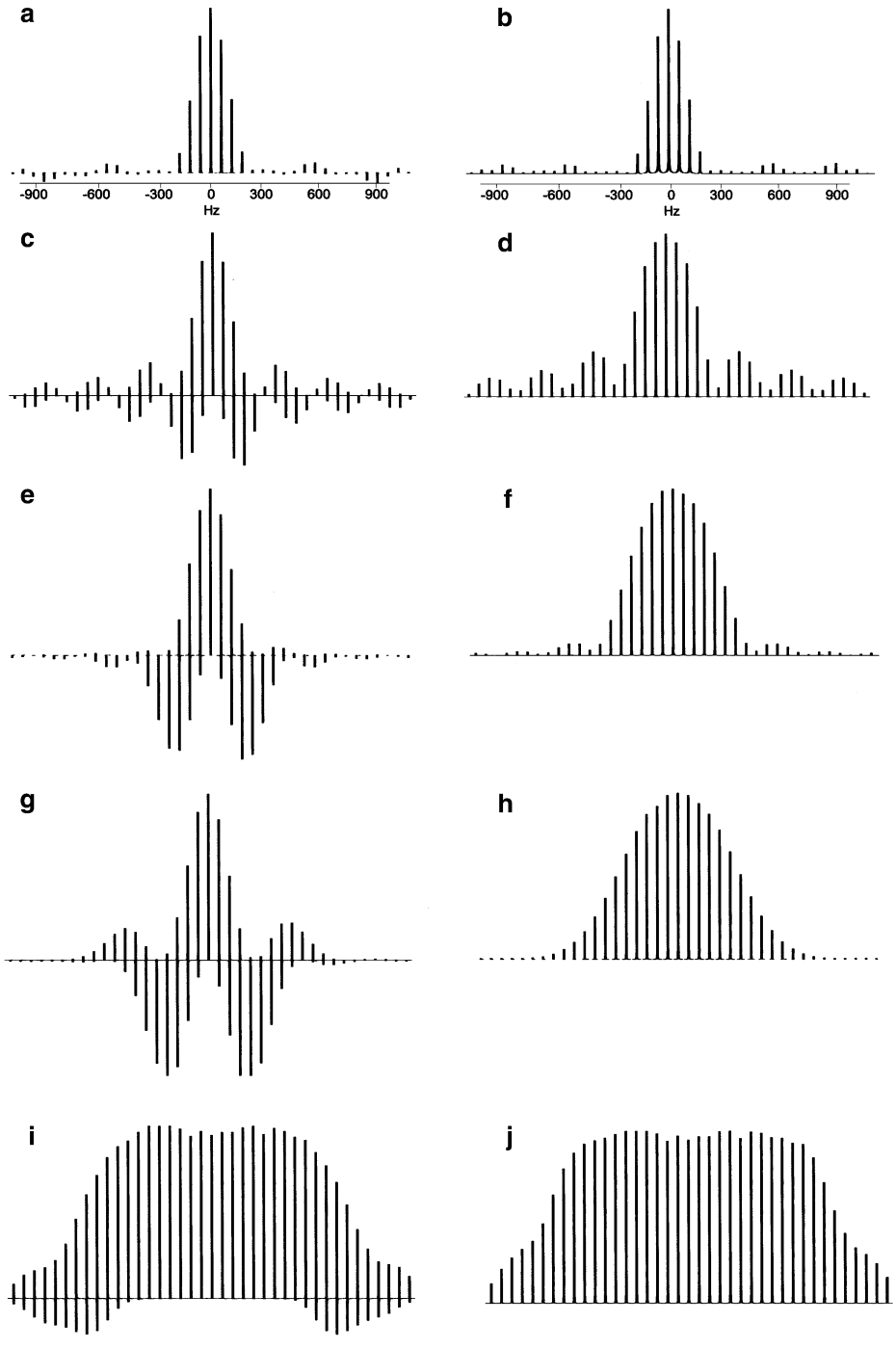

FIG. 3. Experimental excitation profiles (2 kHz wide) of the presented selective excitation scheme in comparison with various shaped-selective pulses. For all pulses the duration was 3.5 ms and both phase-sensitive (left) and absolute value mode (right) profiles are shown. The used pulses are SELDOM pulse cluster (a, b), rectangular soft pulse (c, d), sinc pulse (e, f), Gaussian pulse (g, h), and EBURP2 (i, j). For the same duration, the SELDOM cluster not only gives the narrowest excitation profile, it also shows superior phase behavior compared to all other selective pulses. These profiles were acquired on a H_2O/D_2O (1%/99%) sample doped with $GdCl_3$ (1 mg/ml) to enable faster relaxation.

rectangular (Fig. 3c), sinc (Fig. 3e), and Gaussian (Fig. 3g) pulse shapes. It was verified experimentally (data not shown) that the excitation profiles of DANTE pulse clusters consisting of equal intensity low-power pulses are the same as a rectangular pulse excitation profile of the same duration with sidebands at distances corresponding to the reciprocal of the interpulse delay.

A common parameter for quantifying the selectivity of a selective pulse is the product $\Delta t\,\Delta\Omega$ for a 3-dB decrease of maximum

intensity in the excited signal (*14*). For a SELDOM pulse with four repetitions and a $\tau_{min} = 0.5$ ms and $\tau_{max} = 2.0$ ms this ratio is 0.39 as calculated by Eq. [3]. A comparison with $\Delta t \Delta\Omega$ ratios of several shaped pulses (rectangular, 1.12; Gaussian, 1.32; EBURP2, 5.00) (*14*) clearly shows the superiority of SELDOM if highly selective excitation is needed within a relatively short time. In addition to superior excitation characteristics, the setup of the SELDOM cluster is straightforward since no additional pulse angle determination is necessary. Solely, a regular 90° pulse is needed. The SELDOM scheme is also very robust to pulse angle and phase errors since the hard pulses are alternatively applied from two opposite directions and errors cancel each other out before the gradient is applied. Possible phase coherence problems that are sometimes encountered by using selective excitation units for the generation of shaped low-power pulses are circumvented since all pulses are generated the same way and no special hardware for the creation of shaped low-power pulses is necessary.

To theoretically compare the relaxation losses during the SELDOM scheme compared to various other relaxation optimized pulses for selective excitation, numerical simulations were carried out using the Bloch equations including relaxation,

$$\frac{dM_x}{dt} = -\frac{M_x}{T_2} - M_y\Delta\nu + M_z\gamma B_1 \sin(\phi)$$

$$\frac{dM_y}{dt} = -\frac{M_y}{T_2} + M_x\Delta\nu + M_z\gamma B_1 \cos(\phi) \quad [4]$$

$$\frac{dM_z}{dt} = -\frac{M_0 - M_z}{T_1} - M_x\gamma B_1 \sin(\phi) - M_y\gamma B_1 \cos(\phi),$$

where M_x, M_y, and M_z are the magnetization components in the x, y, and z directions, T_1 is the longitudinal and T_2 the transverse relaxation time, γ is the gyromagnetic ration, ν is the frequency offset, and ϕ is the pulse phase. Figure 4 shows excitation profiles calculated for (a) the SELDOM cluster, (b) a DANTE-Z cluster, (c) an e-SNOB pulse, and (d) a SLURP-2 pulse. The pulse lengths were chosen to produce excitation up to ±100 Hz. The T_1 relaxation time was kept constant at 1 s and T_2 values of 100, 50, 30, and 10 ms were used for each pulse as shown by four excitation profiles for every pulse, where the bottom one corresponds to the shortest T_2 relaxation time. To reduce the amount of excited off-resonance magnetization without randomization of τ_a, more steps of the SELDOM scheme were necessary for this simulation. Despite this fact the SELDOM cluster (Fig. 4a) shows less relaxation losses than each shaped pulse (Figs. 4c and 4d) and less excitation of off-resonance magnetization than the DANTE-z pulse cluster (Fig. 4b). The total duration of the pulses were 4.8 ms for the SELDOM scheme, 8 ms for the DANTE-Z pulse, 15 ms for the e-SNOB, and 30 ms

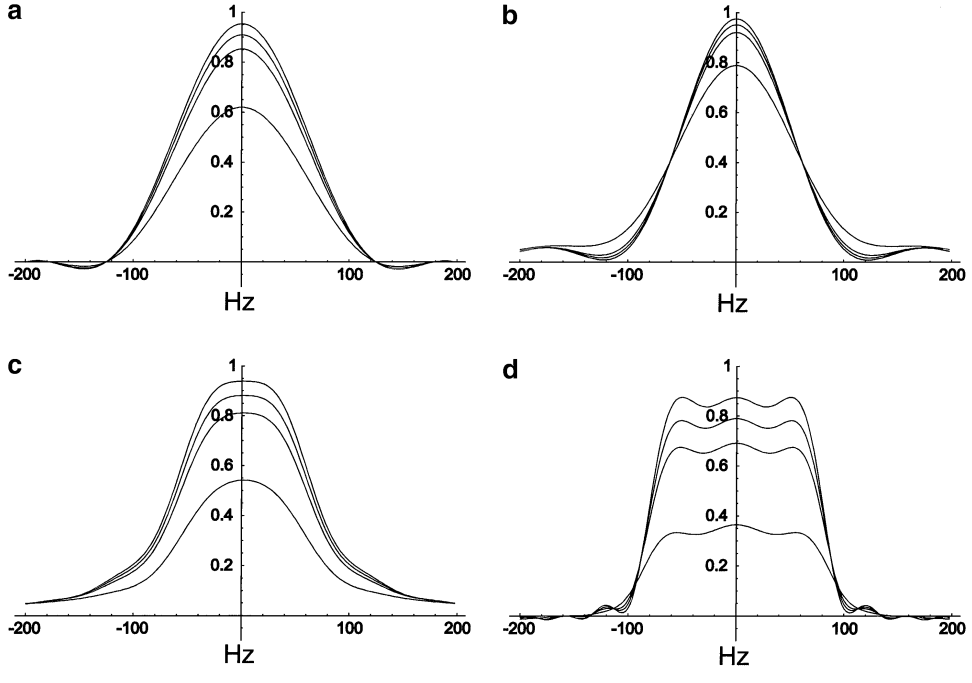

FIG. 4. Theoretical excitation profiles of (a) a SELDOM cluster (4.8 ms), (b) a DANTE-Z pulse (8 ms), (c) an e-SNOB pulse (15 ms), and (d) a SLURP-2 pulse (30 ms) calculated by solving Eqs. [4] numerically. Thereby, $T_1 = 1$ s and T_2 was varied between 100, 50, 30, and 10 ms for each selective pulse. The topmost excitation profile corresponds to the longest and the bottom one to the shortest T_2 relaxation time. The frequency offset is given in hertz and the signal intensity in relative units where 1 stands for maximum signal (excitation with a hard 90° pulse without relaxation). The pulse lengths were chosen to give similar excitation bandwidths for all pulses. Six steps were used for the SELDOM pulse cluster with interpulse delays of 2, 1.4, 1.2, 0.15, 0.1, and 0.01 ms. The DANTE-Z cluster consisted of 40 steps.

for the SLURP-2 pulse. Scalar coupling, which was not included in this calculation, is likely to cause problems for longer pulses.

An experimental comparison of the SELDOM pulse cluster with other relaxation optimized selective pulses is shown in Fig. 5. To selectively excite the signal at -0.15 ppm (indicated in Fig. 5a) of a 3-mM sample of lysozyme ($T_2 = 22$ ms) with the same excitation bandwidth, the durations of the selective pulses used had to be varied: 3.9 ms for the SELDOM cluster (Fig. 5b), 10 ms for the DANTE-Z cluster (Figure 6d), 19 ms for the SNOB (Fig. 6c), and 40 ms for the SLURP-2 (Fig. 6d). The interpulse delay of the SELDOM cluster was varied randomly $\pm 50\%$ for the spectrum in Fig. 5b), which results in a shorter pulse length and still better artifact suppression.

Whenever transverse magnetization is present during the application of a selective pulse, T_2 relaxation occurs. For the SELDOM cluster this is the sum of interpulse delays, whereas for shaped-selective pulses the projection of the magnetization trajectory onto the x, y plane is rather small for the most time (*16*, *18*). However, to achieve sufficient selectivity for shaped pulses, the total time the magnetization spends away from the z axis is still significant and therefore the signal excited with the SELDOM pulse train is still the most intense thanks to the short overall duration.

The relative signal intensities are 100:104:106:123 for SLURP-2:e-SNOB:DANTE-Z:SELDOM. The larger signal intensity obtained by using the SELDOM cluster over the DANTE-Z compared to the results from the theoretical calculation (Fig. 4) probably stems from the smaller number of steps necessary for artifact suppression if τ_a is randomized. Since the DANTE-Z pulse train relies on phase cycling for achieving its selectivity, the receiver gain had to be reduced during the acquisition of all spectra in Fig. 5 to allow for a fair comparison. This might prevent the use of DANTE-Z pulse clusters in systems with very large signals (e.g., from the solvent) due to dynamic range problems.

It is worth mentioning that multiple excitation could also be achieved with the SELDOM pulse cluster. Incrementing τ_a in constant steps of τ_{min} produces excitation sidebands at frequencies separated by $1/\tau_{min}$.

The selective excitation by the SELDOM scheme can also be implemented into the direct or indirect dimensions of multidimensional NMR experiments (Fig. 1c). As an example of the usage of the SELDOM pulse cluster within a pulse sequence, Fig. 6 shows the selective excitation of a single amide proton in ^{15}N-labeled 19-kD dimeric protein ParD through simultaneous ^{1}H and ^{15}N selective excitation of the cross peak indicated in Fig. 6a. As mentioned above, scalar coupling between the proton and its directly attached ^{15}N nucleus is not active during the SELDOM scheme since only zero- and double-quantum magnetization is present during the delays of free precession. The selectively excited signal is only about 60 Hz separated from its closest neighbor in the nitrogen dimension. Due to the large

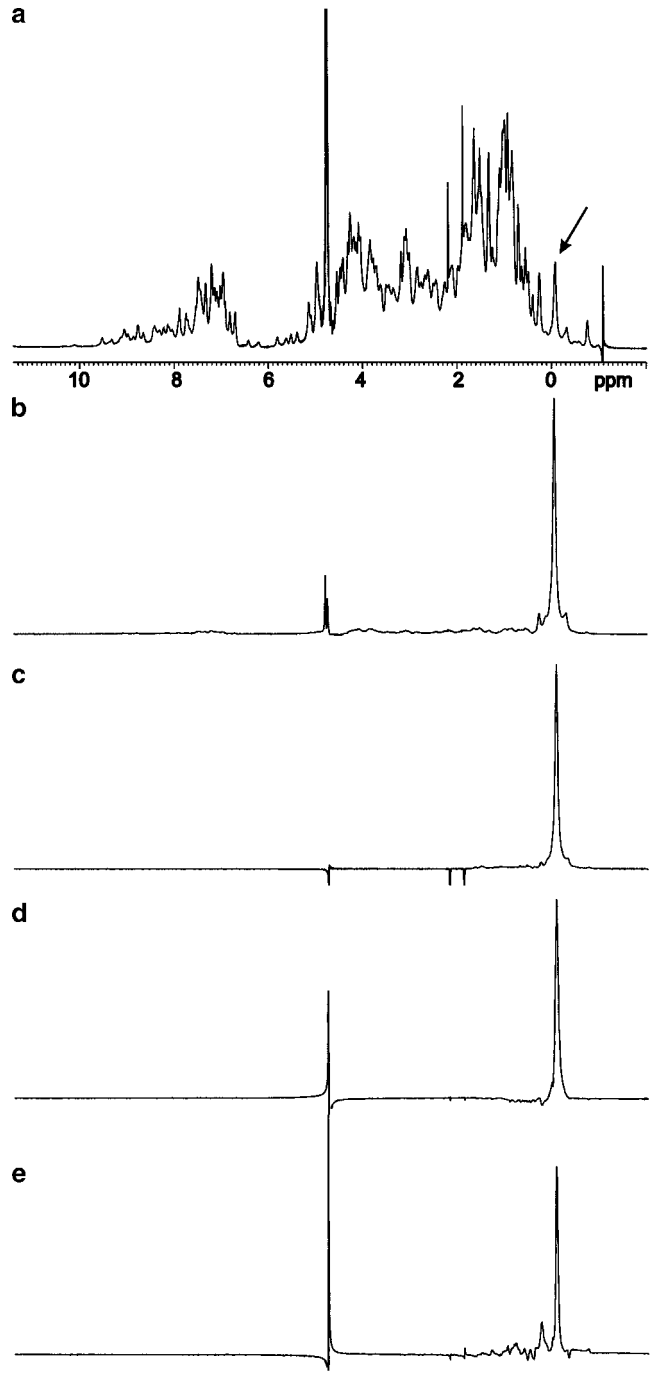

FIG. 5. (a) One-dimensional ^{1}H-NMR spectrum of lysozyme in D_2O and the signal at -0.15 ppm (indicated by an arrow) selectively excited with selective pulses of the same bandwidth, using (b) a 3.9-ms SELDOM cluster, (c) a 10-ms DANTE-Z pulse cluster, (d) a 19-ms SNOB pulse, and (e) a 40-ms SLURP-2 pulse. The spectra (b–e) are drawn with the same vertical scale to allow a direct comparison of signal intensities, whereas the intensity of the regular 1D spectrum (a) is reduced by a factor of 4 to enable an estimation of signal amplitudes in the whole spectrum. A total of 128 transients were accumulated for each spectrum and the FIDs were multiplied by an exponential window function with a line-broadening of 2 Hz prior to Fourier transformation. Five steps were used for the SELDOM pulse cluster and the interpulse delays of 1.5, 0.9, 0.7, 0.5, and 0.3 ms varied randomly by $\pm 50\%$. The DANTE-Z cluster consisted of 40 steps.

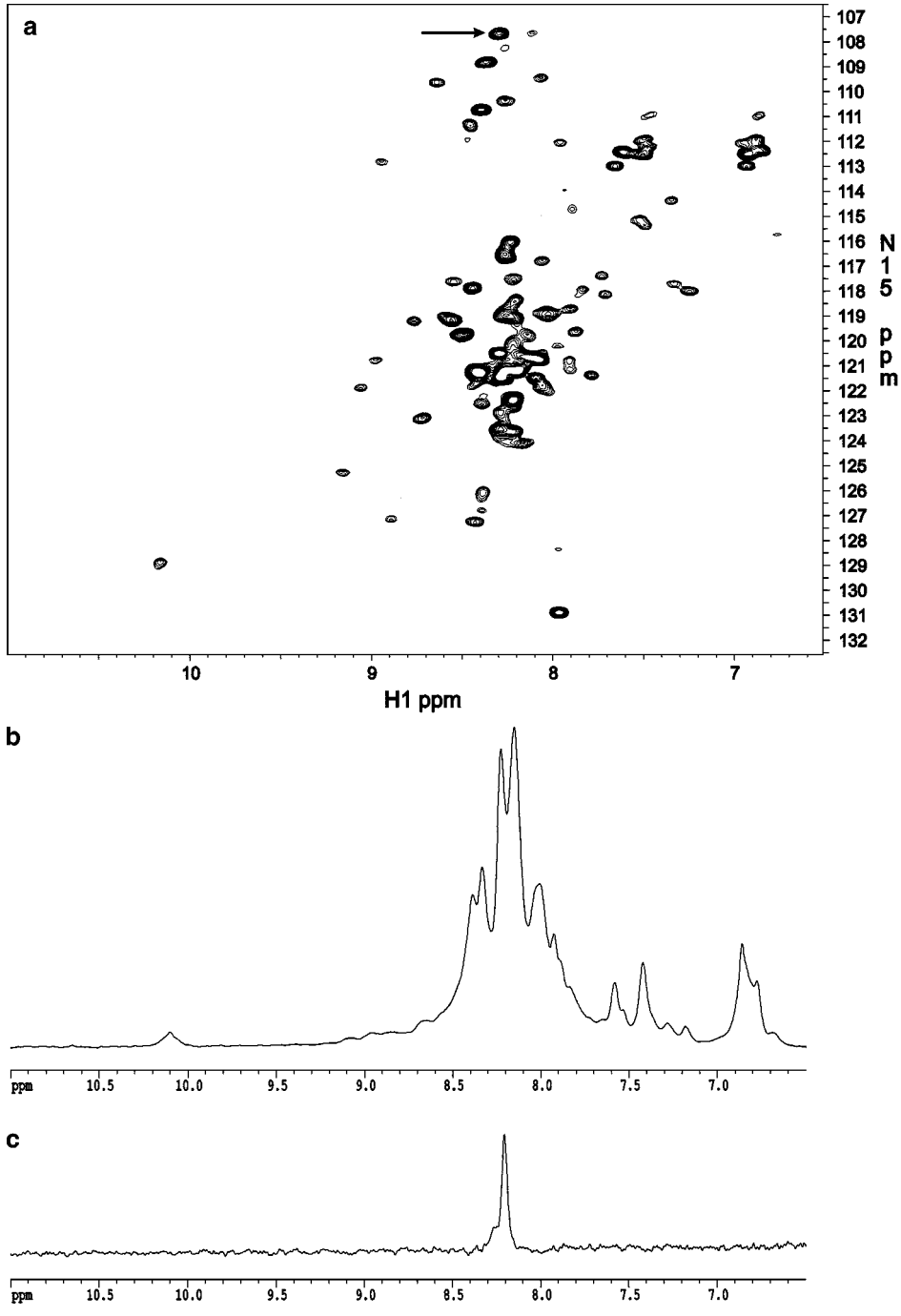

FIG. 6. (a) A 2D ^{1}H–^{15}N HSQC of ^{15}N-labeled ParD, (b) a 1D ^{1}H–^{15}N HSQC of the same sample, and (c) a double-selective 1D ^{1}H–^{15}N HSQC obtained by selective excitation of the signal indicated in (a) using the pulse sequence shown in Fig. 1c. Thirty-two scans of 1024 complex data points were acquired for each of the 128 increments for (a). After multiplying the FIDs with a 60° phase-shifted squared cosine window function in both dimensions the data were zero-filled to a final matrix of 2K × 1K points. For (b) and (c) 1024 transients were accumulated and multiplied with a 60° phase-shifted squared cosine window function prior to Fourier transformation. For (b) an exponential window function with 10-Hz line broadening was applied additionally. The interpulse delays were varied randomly by ±30%. Four repetitions of the SELDOM pulse cluster with a total duration of 5 ms were used for the selective excitation in (c).

one-bond H–N coupling (∼90 Hz) it would not be possible to selectively excite this signal using regular selective pulses.

In conclusion, a new method for selective excitation in fast-relaxing systems has been presented. It works by defocusing the off-resonance magnetization, created during subsequent delays of free precession, with pulsed field gradients and allows a highly selective excitation without dispersive components within a short time. It is especially suited for double-selective excitation of H–X scalar-coupled spins due to the elimination of scalar coupling during the pulse cluster. Its superiority in selectivity as well as relaxation and phase behavior has been shown theoretically, as well as experimentally, for proteins ranging in size between 14 and 19 kD.

EXPERIMENTAL

All experiments were carried out on a Bruker Avance 500-MHz NMR spectrometer equipped with *z*-axis gradients using a 5-mm H*X* inverse probe except for the experimental excitation profiles that were recorded on a Varian Unity INOVA 600-MHz NMR spectrometer. A solution of 3 mM lysozyme in D_2O at pH 7.0 was used at 25°C. Under these conditions the transverse relaxation time (T_2) of the selectively excited signal was 22 ms. ^{15}N-labeled ParD was expressed in minimal media with 15 g/l $(NH_4)_2SO_4$ as the sole nitrogen source in *E. Coli* BL21 essentially as described (*27*). A sample of 0.7 mM ^{15}N-labeled ParD in H_2O/D_2O (90%/10%), 20 mM phosphate buffer, pH 6.0 was used. The transverse relaxation time of the selectively excited amide signal in ParD was around 18 ms. Experimental excitation profiles were obtained on 1% H_2O in D_2O solutions doped with GdCl3 (1 mg/ml). If not stated otherwise, the interpulse delay τ_a was incremented in equal steps of $(\tau_{max} - \tau_{min})/(n - 1)$, where τ_{max} and τ_{min} are the maximum and minimum interpulse delays and n is the number of repetitions. Eight repetitions of the SELDOM cluster were used for the experimental excitation profiles on the doped H_2O sample. The gradient strengths were not changed in a random fashion but instead varied according to ratios of $1:1.12:1.34:1.76:1.21:1.43:1.67:1.89$ for all the experimental spectra shown. Details of the processing and display schemes are given in the figure captions. All calculations were carried out with Mathematica (*28*).

ACKNOWLEDGMENTS

K.Z. thanks the Austrian Academy of Sciences for an APART fellowship. Partial support of this work by the Austrian Fonds zur Förderung der wissenschaftlichen Forschung (Project Number P13909CHE) to H.S. is gratefully acknowledged.

REFERENCES

1. R. R. Ernst, G. Bodenhausen, and A. Wokaun, "Principles of Nuclear Magnetic Resonance in One and Two Dimensions," Clarendon Press, Oxford (1994).
2. L. Emsley and G. Bodenhausen, Self-refocusing effect of 270 degrees Gaussian pulses—Application to selective two-dimensional exchange spectroscopy, *J. Magn. Reson*. **82,** 211–221 (1989).
3. R. Freeman, Slective excitation in high-resolution NMR, *Chem. Rev*. **91,** 1397–1412 (1991).
4. H. Kessler, C. Griesinger, and H. Oschkinat, Transformation of homonuclear two-dimensional NMR techniques into one-dimensional techniques using Gaussian pulses, *J. Magn. Reson*. **70,** 106–133 (1986).
5. H. Kessler, U. Anders, G. Gemmecker, and S. Steuernagel, Improvements of NMR experiments by employing semiselective half-Gaussian-shaped pulses, *J. Magn. Reson*. **85,** 1–14 (1989).
6. H. Kessler, S. Mronga, and G. Gemmecker, Multidimensional NMR experiments using selective pulses, *Magn. Reson. Chem*. **29,** 527–557 (1991).
7. G. A. Morris and R. Freeman, Selective excitation in Fourier transform nuclear magnetic resonance, *J. Magn. Reson*. **29,** 433–462 (1978).
8. D. I. Hoult, C.-N. Chen, H. Eden, and M. Eden, Elimination of baseline artifacts in spectra and their integrals, *J. Magn. Reson*. **51,** 110–117 (1983).
9. J. Cavanagh, W. J. Fairbrother, A. G. Palmer, and N. J. Skelton, "Protein NMR Spectroscopy," Academic Press, San Diego (1996).
10. M. Piotto, V. Saudek, and V. Sklenar, Gradient-tailored excitation for single-quantum NMR spectroscopy of aqueous solutions, *J. Biomol. NMR* **2,** 661–665 (1992).
11. E. Chiarparin, P. Pelupessy, P. Cutting, T. R. Eykyn, and G. Bodenhausen, Normalized one-dimensional NOE measurements in isotopically labeled macromoleculesusing 2-way cross-polarization, *J. Biomol. NMR* **13,** 61–65 (1999).
12. T. R. Eykyn, R. Ghose, and G. Bodenhausen, Offset profiles of selective pulses in isotopically labeled macromolecules, *J. Magn. Reson*. **136,** 211–213 (1999).
13. P. Pelupessy, E. Chiarparin, and G. Bodenhausen, Excitation of selected proton signals in NMR of isotopically labeled macromolecules, *J. Magn. Reson*. **138,** 178–81 (1999).
14. P. J. Hajduk, D. A. Horita, and L. E. Lerner, Theoretical analysis of relaxation during shaped pulses. I. The effects of short T1 and T2, *J. Magn. Reson. A* **103,** 40–52 (1993).
15. D. A. Horita, P. J. Hajduk, and L. E. Lerner, Theoretical analysis of relaxation during shaped pulses. II. The effect of cross relaxation, *J. Magn. Reson. A* **103,** 53–60 (1993).
16. H. Geen and R. Freeman, Band-selective radiofrequency pulses, *J. Magn. Reson*. **93,** 93–141 (1991).
17. E. Kupce, J. Boyd, and I. D. Campbell, Short selective pulses for biochemical applications, *J. Magn. Reson. B* **106,** 300–303 (1995).
18. J.-M. Nuzillard and R. Freeman, Band-selective pulses designed to accomodate relaxation, *J. Magn. Reson. A* **107,** 113–118 (1994).
19. C. Roumestand, D. Canet, N. Mahieu, and F. Toma, DANTE-Z, an alternative to low-power soft pulses. Improvement of the selection scheme and applications to multidimensional NMR studies of proteins, *J. Magn. Reson. A* **106,** 168–181 (1994).
20. D. Boudot, D. Canet, J. Brondeau, and J. C. Boubel, DANTE-Z. A new approach for accurate frequency selectivity using hard pulses, *J. Magn. Reson*. **83,** 428–439 (1989).
21. G. Bodenhausen and D. J. Ruben, Natural abundance N-15 NMR by enhanced heteronuclear spectroscopy, *Chem. Phys. Lett*. **69,** 185 (1980).
22. A. J. Shaka and R. Freeman, Spatially selective pulse sequences: Elimination of harmonic responses, *J. Magn. Reson*. **62,** 340–345 (1985).

23. A. J. Shaka and R. Freeman, "Prepulses" for spatial localization, *J. Magn. Reson*. **64,** 145–150 (1985).

24. K. Stott, J. Stonehouse, J. Keeler, T.-L. Hwang, and A. J. Shaka, Excitation sculpting in high-resolution nuclear-magnetic-resonance spectroscopy. Application to selective NOE experiments, *J. Am. Chem. Soc*. **117,** 4199–4200 (1995).

25. K. Stott, J. Keeler, Q. N. Van, and A. J. Shaka, One-dimensional NOE experiments using pulsed field gradients, *J. Magn. Reson.* **125,** 302–324 (1997).

26. T.-L. Hwang and A. J. Shaka, Water suppression that works. Excitation sculpting using arbitrary waveforms and pulsed field gradients, *J. Magn. Reson. A* **112,** 275–279 (1995).

27. M. Oberer, H. Lindner, O. Glatter, C. Kratky, and W. Keller, Thermodynamic properties and DNA binding of the ParD protein from the broad host-range plasmid RK2/RP4 killing system, *Biol. Chem.* **380,** 1413–1420 (1999).

28. S. Wolfram, "*Mathematica*," 4.0 ed., Wolfram Research Inc., Champaign, IL (1999).